

## Search for lepton flavor violating $\tau \rightarrow \ell V^0$ decays at Belle

K. Abe,<sup>10</sup> I. Adachi,<sup>10</sup> H. Aihara,<sup>52</sup> K. Arinstein,<sup>1</sup> T. Aso,<sup>56</sup> V. Aulchenko,<sup>1</sup> T. Aushev,<sup>22,16</sup> T. Aziz,<sup>48</sup> S. Bahinipati,<sup>3</sup> A. M. Bakich,<sup>47</sup> V. Balagura,<sup>16</sup> Y. Ban,<sup>38</sup> S. Banerjee,<sup>48</sup> E. Barberio,<sup>25</sup> A. Bay,<sup>22</sup> I. Bedny,<sup>1</sup> K. Belous,<sup>15</sup> V. Bhardwaj,<sup>37</sup> U. Bitenc,<sup>17</sup> S. Blyth,<sup>29</sup> A. Bondar,<sup>1</sup> A. Bozek,<sup>31</sup> M. Bračko,<sup>24,17</sup> J. Brodzicka,<sup>10</sup> T. E. Browder,<sup>9</sup> M.-C. Chang,<sup>4</sup> P. Chang,<sup>30</sup> Y. Chao,<sup>30</sup> A. Chen,<sup>28</sup> K.-F. Chen,<sup>30</sup> W. T. Chen,<sup>28</sup> B. G. Cheon,<sup>8</sup> C.-C. Chiang,<sup>30</sup> R. Chistov,<sup>16</sup> I.-S. Cho,<sup>58</sup> S.-K. Choi,<sup>7</sup> Y. Choi,<sup>46</sup> Y. K. Choi,<sup>46</sup> S. Cole,<sup>47</sup> J. Dalseno,<sup>25</sup> M. Danilov,<sup>16</sup> A. Das,<sup>48</sup> M. Dash,<sup>57</sup> J. Dragic,<sup>10</sup> A. Drutskoy,<sup>3</sup> S. Eidelman,<sup>1</sup> D. Epifanov,<sup>1</sup> S. Fratina,<sup>17</sup> H. Fujii,<sup>10</sup> M. Fujikawa,<sup>27</sup> N. Gabyshev,<sup>1</sup> A. Garmash,<sup>40</sup> A. Go,<sup>28</sup> G. Gokhroo,<sup>48</sup> P. Goldenzweig,<sup>3</sup> B. Golob,<sup>23,17</sup> M. Grosse Perdekamp,<sup>12,41</sup> H. Guler,<sup>9</sup> H. Ha,<sup>19</sup> J. Haba,<sup>10</sup> K. Hara,<sup>26</sup> T. Hara,<sup>36</sup> Y. Hasegawa,<sup>45</sup> N. C. Hastings,<sup>52</sup> K. Hayasaka,<sup>26</sup> H. Hayashii,<sup>27</sup> M. Hazumi,<sup>10</sup> D. Heffernan,<sup>36</sup> T. Higuchi,<sup>10</sup> L. Hinz,<sup>22</sup> H. Hoedlmoser,<sup>9</sup> T. Hokuue,<sup>26</sup> Y. Horii,<sup>51</sup> Y. Hoshi,<sup>50</sup> K. Hoshina,<sup>55</sup> S. Hou,<sup>28</sup> W.-S. Hou,<sup>30</sup> Y. B. Hsiung,<sup>30</sup> H. J. Hyun,<sup>21</sup> Y. Igarashi,<sup>10</sup> T. Iijima,<sup>26</sup> K. Ikado,<sup>26</sup> K. Inami,<sup>26</sup> A. Ishikawa,<sup>42</sup> H. Ishino,<sup>53</sup> R. Itoh,<sup>10</sup> M. Iwabuchi,<sup>6</sup> M. Iwasaki,<sup>52</sup> Y. Iwasaki,<sup>10</sup> C. Jacoby,<sup>22</sup> N. J. Joshi,<sup>48</sup> M. Kaga,<sup>26</sup> D. H. Kah,<sup>21</sup> H. Kajii,<sup>26</sup> S. Kajiwara,<sup>36</sup> H. Kakuno,<sup>52</sup> J. H. Kang,<sup>58</sup> P. Kapusta,<sup>31</sup> S. U. Kataoka,<sup>27</sup> N. Katayama,<sup>10</sup> H. Kawai,<sup>2</sup> T. Kawasaki,<sup>33</sup> A. Kibayashi,<sup>10</sup> H. Kichimi,<sup>10</sup> H. J. Kim,<sup>21</sup> H. O. Kim,<sup>46</sup> J. H. Kim,<sup>46</sup> S. K. Kim,<sup>44</sup> Y. J. Kim,<sup>6</sup> K. Kinoshita,<sup>3</sup> S. Korpar,<sup>24,17</sup> Y. Kozakai,<sup>26</sup> P. Križan,<sup>23,17</sup> P. Krokovny,<sup>10</sup> R. Kumar,<sup>37</sup> E. Kurihara,<sup>2</sup> A. Kusaka,<sup>52</sup> A. Kuzmin,<sup>1</sup> Y.-J. Kwon,<sup>58</sup> J. S. Lange,<sup>5</sup> G. Leder,<sup>14</sup> J. Lee,<sup>44</sup> J. S. Lee,<sup>46</sup> M. J. Lee,<sup>44</sup> S. E. Lee,<sup>44</sup> T. Lesiak,<sup>31</sup> J. Li,<sup>9</sup> A. Limosani,<sup>25</sup> S.-W. Lin,<sup>30</sup> Y. Liu,<sup>6</sup> D. Liventsev,<sup>16</sup> J. MacNaughton,<sup>10</sup> G. Majumder,<sup>48</sup> F. Mandl,<sup>14</sup> D. Marlow,<sup>40</sup> T. Matsumura,<sup>26</sup> A. Matyja,<sup>31</sup> S. McOnie,<sup>47</sup> T. Medvedeva,<sup>16</sup> Y. Mikami,<sup>51</sup> W. Mitaroff,<sup>14</sup> K. Miyabayashi,<sup>27</sup> H. Miyake,<sup>36</sup> H. Miyata,<sup>33</sup> Y. Miyazaki,<sup>26</sup> R. Mizuk,<sup>16</sup> G. R. Moloney,<sup>25</sup> T. Mori,<sup>26</sup> J. Mueller,<sup>39</sup> A. Murakami,<sup>42</sup> T. Nagamine,<sup>51</sup> Y. Nagasaka,<sup>11</sup> Y. Nakahama,<sup>52</sup> I. Nakamura,<sup>10</sup> E. Nakano,<sup>35</sup> M. Nakao,<sup>10</sup> H. Nakayama,<sup>52</sup> H. Nakazawa,<sup>28</sup> Z. Natkaniec,<sup>31</sup> K. Neichi,<sup>50</sup> S. Nishida,<sup>10</sup> K. Nishimura,<sup>9</sup> Y. Nishio,<sup>26</sup> I. Nishizawa,<sup>54</sup> O. Nitoh,<sup>55</sup> S. Noguchi,<sup>27</sup> T. Nozaki,<sup>10</sup> A. Ogawa,<sup>41</sup> S. Ogawa,<sup>49</sup> T. Ohshima,<sup>26</sup> S. Okuno,<sup>18</sup> S. L. Olsen,<sup>9</sup> S. Ono,<sup>53</sup> W. Ostrowicz,<sup>31</sup> H. Ozaki,<sup>10</sup> P. Pakhlov,<sup>16</sup> G. Pakhlova,<sup>16</sup> H. Palka,<sup>31</sup> C. W. Park,<sup>46</sup> H. Park,<sup>21</sup> K. S. Park,<sup>46</sup> N. Parslow,<sup>47</sup> L. S. Peak,<sup>47</sup> M. Pernicka,<sup>14</sup> R. Pestotnik,<sup>17</sup> M. Peters,<sup>9</sup> L. E. Piilonen,<sup>57</sup> A. Poluektov,<sup>1</sup> J. Rorie,<sup>9</sup> M. Rozanska,<sup>31</sup> H. Sahoo,<sup>9</sup> Y. Sakai,<sup>10</sup> H. Sakaue,<sup>35</sup> N. Sasao,<sup>20</sup> T. R. Sarangi,<sup>6</sup> N. Satoyama,<sup>45</sup> K. Sayeed,<sup>3</sup> T. Schietinger,<sup>22</sup> O. Schneider,<sup>22</sup> P. Schönmeier,<sup>51</sup> J. Schümann,<sup>10</sup> C. Schwanda,<sup>14</sup> A. J. Schwartz,<sup>3</sup> R. Seidl,<sup>12,41</sup> A. Sekiya,<sup>27</sup> K. Senyo,<sup>26</sup> M. E. Sevier,<sup>25</sup> L. Shang,<sup>13</sup> M. Shapkin,<sup>15</sup> C. P. Shen,<sup>13</sup> H. Shibuya,<sup>49</sup> S. Shinomiya,<sup>36</sup> J.-G. Shiu,<sup>30</sup> B. Shwartz,<sup>1</sup> J. B. Singh,<sup>37</sup> A. Sokolov,<sup>15</sup> E. Solovieva,<sup>16</sup> A. Somov,<sup>3</sup> S. Stanič,<sup>34</sup> M. Starič,<sup>17</sup> J. Stypula,<sup>31</sup> A. Sugiyama,<sup>42</sup> K. Sumisawa,<sup>10</sup> T. Sumiyoshi,<sup>54</sup> S. Suzuki,<sup>42</sup> S. Y. Suzuki,<sup>10</sup> O. Tajima,<sup>10</sup> F. Takasaki,<sup>10</sup> K. Tamai,<sup>10</sup> N. Tamura,<sup>33</sup> M. Tanaka,<sup>10</sup> N. Taniguchi,<sup>20</sup> G. N. Taylor,<sup>25</sup> Y. Teramoto,<sup>35</sup> I. Tikhomirov,<sup>16</sup> K. Trabelsi,<sup>10</sup> Y. F. Tse,<sup>25</sup> T. Tsuboyama,<sup>10</sup> K. Uchida,<sup>9</sup> Y. Uchida,<sup>6</sup> S. Uehara,<sup>10</sup> K. Ueno,<sup>30</sup> T. Uglov,<sup>16</sup> Y. Unno,<sup>8</sup> S. Uno,<sup>10</sup> P. Urquijo,<sup>25</sup> Y. Ushiroda,<sup>10</sup> Y. Usov,<sup>1</sup> G. Varner,<sup>9</sup> K. E. Varvell,<sup>47</sup> K. Vervink,<sup>22</sup> S. Villa,<sup>22</sup> A. Vinokurova,<sup>1</sup> C. C. Wang,<sup>30</sup> C. H. Wang,<sup>29</sup> J. Wang,<sup>38</sup> M.-Z. Wang,<sup>30</sup> P. Wang,<sup>13</sup> X. L. Wang,<sup>13</sup> M. Watanabe,<sup>33</sup> Y. Watanabe,<sup>18</sup> R. Wedd,<sup>25</sup> J. Wicht,<sup>22</sup> L. Widhalm,<sup>14</sup> J. Wiechczynski,<sup>31</sup> E. Won,<sup>19</sup> B. D. Yabsley,<sup>47</sup> A. Yamaguchi,<sup>51</sup> H. Yamamoto,<sup>51</sup> M. Yamaoka,<sup>26</sup> Y. Yamashita,<sup>32</sup> M. Yamauchi,<sup>10</sup> C. Z. Yuan,<sup>13</sup> Y. Yusa,<sup>57</sup> C. C. Zhang,<sup>13</sup> L. M. Zhang,<sup>43</sup> Z. P. Zhang,<sup>43</sup> V. Zhilich,<sup>1</sup> V. Zhulanov,<sup>1</sup> A. Zupanc,<sup>17</sup> and N. Zwahlen<sup>22</sup>

(The Belle Collaboration)

<sup>1</sup>*Budker Institute of Nuclear Physics, Novosibirsk*

<sup>2</sup>*Chiba University, Chiba*

<sup>3</sup>*University of Cincinnati, Cincinnati, Ohio 45221*

<sup>4</sup>*Department of Physics, Fu Jen Catholic University, Taipei*

<sup>5</sup>*Justus-Liebig-Universität Gießen, Gießen*

<sup>6</sup>*The Graduate University for Advanced Studies, Hayama*

<sup>7</sup>*Gyeongsang National University, Chinju*

<sup>8</sup>*Hanyang University, Seoul*

<sup>9</sup>*University of Hawaii, Honolulu, Hawaii 96822*

<sup>10</sup>*High Energy Accelerator Research Organization (KEK), Tsukuba*

<sup>11</sup>*Hiroshima Institute of Technology, Hiroshima*

<sup>12</sup>*University of Illinois at Urbana-Champaign, Urbana, Illinois 61801*

- <sup>13</sup>*Institute of High Energy Physics, Chinese Academy of Sciences, Beijing*  
<sup>14</sup>*Institute of High Energy Physics, Vienna*  
<sup>15</sup>*Institute of High Energy Physics, Protvino*  
<sup>16</sup>*Institute for Theoretical and Experimental Physics, Moscow*  
<sup>17</sup>*J. Stefan Institute, Ljubljana*  
<sup>18</sup>*Kanagawa University, Yokohama*  
<sup>19</sup>*Korea University, Seoul*  
<sup>20</sup>*Kyoto University, Kyoto*  
<sup>21</sup>*Kyungpook National University, Taegu*  
<sup>22</sup>*École Polytechnique Fédérale de Lausanne (EPFL), Lausanne*  
<sup>23</sup>*University of Ljubljana, Ljubljana*  
<sup>24</sup>*University of Maribor, Maribor*  
<sup>25</sup>*University of Melbourne, School of Physics, Victoria 3010*  
<sup>26</sup>*Nagoya University, Nagoya*  
<sup>27</sup>*Nara Women's University, Nara*  
<sup>28</sup>*National Central University, Chung-li*  
<sup>29</sup>*National United University, Miao Li*  
<sup>30</sup>*Department of Physics, National Taiwan University, Taipei*  
<sup>31</sup>*H. Niewodniczanski Institute of Nuclear Physics, Krakow*  
<sup>32</sup>*Nippon Dental University, Niigata*  
<sup>33</sup>*Niigata University, Niigata*  
<sup>34</sup>*University of Nova Gorica, Nova Gorica*  
<sup>35</sup>*Osaka City University, Osaka*  
<sup>36</sup>*Osaka University, Osaka*  
<sup>37</sup>*Panjab University, Chandigarh*  
<sup>38</sup>*Peking University, Beijing*  
<sup>39</sup>*University of Pittsburgh, Pittsburgh, Pennsylvania 15260*  
<sup>40</sup>*Princeton University, Princeton, New Jersey 08544*  
<sup>41</sup>*RIKEN BNL Research Center, Upton, New York 11973*  
<sup>42</sup>*Saga University, Saga*  
<sup>43</sup>*University of Science and Technology of China, Hefei*  
<sup>44</sup>*Seoul National University, Seoul*  
<sup>45</sup>*Shinshu University, Nagano*  
<sup>46</sup>*Sungkyunkwan University, Suwon*  
<sup>47</sup>*University of Sydney, Sydney, New South Wales*  
<sup>48</sup>*Tata Institute of Fundamental Research, Mumbai*  
<sup>49</sup>*Toho University, Funabashi*  
<sup>50</sup>*Tohoku Gakuin University, Tagajo*  
<sup>51</sup>*Tohoku University, Sendai*  
<sup>52</sup>*Department of Physics, University of Tokyo, Tokyo*  
<sup>53</sup>*Tokyo Institute of Technology, Tokyo*  
<sup>54</sup>*Tokyo Metropolitan University, Tokyo*  
<sup>55</sup>*Tokyo University of Agriculture and Technology, Tokyo*  
<sup>56</sup>*Toyama National College of Maritime Technology, Toyama*  
<sup>57</sup>*Virginia Polytechnic Institute and State University, Blacksburg, Virginia 24061*  
<sup>58</sup>*Yonsei University, Seoul*

We have searched for neutrinoless  $\tau$  lepton decays into  $\ell$  and  $V^0$ , where  $\ell$  stands for an electron or muon, and  $V^0$  for a vector meson ( $\phi$ ,  $\omega$ ,  $K^{*0}$  or  $\bar{K}^{*0}$ ), using  $543 \text{ fb}^{-1}$  of data collected with the Belle detector at the KEKB asymmetric-energy  $e^+e^-$  collider. No excess of signal events over the expected background is observed, and we set upper limits on the branching fractions in the range  $(0.7 - 1.8) \times 10^{-7}$  at the 90% confidence level. These upper limits include the first results for  $\ell\omega$  as well as new limits that are 3.6 – 9.6 times more restrictive than our previous results for  $\ell\phi$ ,  $\ell K^{*0}$  and  $\ell\bar{K}^{*0}$ .

PACS numbers:

## INTRODUCTION

In the Standard Model (SM), lepton-flavor-violating (LFV) decays of charged leptons are forbidden; even if neutrino mixing is taken into account, they are still highly suppressed. However, LFV is expected to appear

in many extensions of the SM. Some such models predict branching fractions for  $\tau$  LFV decays at the level of  $10^{-8} - 10^{-7}$  [1, 2, 3], which can be reached at the present B-factories. Observation of LFV will then provide evidence for new physics beyond the SM.

In this paper, we report on a search for LFV in  $\tau^-$  de-

cays into neutrinoless final states with one charged lepton  $\ell^-$  and one vector meson  $V^0$ :  $e^-\phi$ ,  $e^-\omega$ ,  $e^-K^{*0}$ ,  $e^-\bar{K}^{*0}$ ,  $\mu^-\phi$ ,  $\mu^-\omega$ ,  $\mu^-K^{*0}$  and  $\mu^-\bar{K}^{*0}$  [4]. A search for the  $\ell^-\phi$ ,  $\ell^-K^{*0}$  and  $\ell^-\bar{K}^{*0}$  modes was performed for the first time at the CLEO detector, where 90% confidence level (CL) upper limits (UL) for the branching fractions in the range  $(5.1 - 7.5) \times 10^{-6}$  were obtained using a data sample of  $4.79 \text{ fb}^{-1}$  [5]. Later we carried out a search for these modes in the Belle experiment using  $158 \text{ fb}^{-1}$  of data and set upper limits in the range  $(3.0 - 7.7) \times 10^{-7}$  [6]. Here we present results of a new search based on a data sample of  $543 \text{ fb}^{-1}$  corresponding to  $4.99 \times 10^8$   $\tau$ -pairs collected with the Belle detector [7] at the KEKB asymmetric-energy  $e^+e^-$  collider [8].

The Belle detector is a large-solid-angle magnetic spectrometer that consists of a silicon vertex detector, a 50-layer central drift chamber, an array of aerogel threshold Cherenkov counters, a barrel-like arrangement of time-of-flight scintillation counters, and an electromagnetic calorimeter comprised of CsI(Tl) crystals located inside a superconducting solenoid coil that provides a 1.5 T magnetic field. An iron flux-return located outside the coil is instrumented to detect  $K_L^0$  mesons and identify muons. The detector is described in detail elsewhere [7]. Two inner detector configurations were used. A 2.0 cm radius beam-pipe and a 3-layer silicon vertex detector were used for the first sample of  $158 \text{ fb}^{-1}$ , while a 1.5 cm radius beam-pipe, a 4-layer silicon detector and a small-cell inner drift chamber were used to record the remaining  $385 \text{ fb}^{-1}$  [9].

## EVENT SELECTION

We search for  $\tau \rightarrow \ell\phi$ ,  $\ell\omega$ ,  $\ell K^{*0}$  and  $\ell\bar{K}^{*0}$  candidates in which one  $\tau$  decays into a final state with a  $\ell$ , two charged hadrons (3-prong decay), and the other  $\tau$  decays into one charged particle (1-prong decay), any number of  $\gamma$ 's and missing particle(s). We reconstruct  $\phi$  candidates from  $K^+K^-$ ,  $\omega$  from  $\pi^+\pi^-\pi^0$ ,  $K^{*0}$  from  $K^+\pi^-$  and  $\bar{K}^{*0}$  from  $K^-\pi^+$ .

The selection criteria described below are optimized from studies of Monte Carlo (MC) simulated events and the experimental data in the sideband regions of the  $\Delta E$  and  $M_{\text{inv}}$  distributions described later. The background (BG) MC samples consist of  $\tau^+\tau^-$  ( $1524 \text{ fb}^{-1}$ ) generated by KKMC [10],  $q\bar{q}$  continuum, and two-photon processes. The signal MC events are generated assuming a phase space distribution for  $\tau$  decay.

The transverse momentum for a charged track is required to be larger than  $0.06 \text{ GeV}/c$  in the barrel region ( $-0.6235 < \cos\theta < 0.8332$ , where  $\theta$  is the polar angle relative to the direction opposite to that of the incident  $e^+$  beam in the laboratory frame) and  $0.1 \text{ GeV}/c$  in the endcap region ( $-0.8660 < \cos\theta < -0.6235$  and  $0.8332 < \cos\theta < 0.9563$ ). The energies of photon can-

didates are required to be larger than  $0.1 \text{ GeV}$  in both regions.

To select the signal topology, we require four charged tracks in an event with zero net charge, and a total energy of charged tracks and photons in the center-of-mass (CM) frame less than  $11 \text{ GeV}$ . We also require that the missing momentum in the laboratory frame be greater than  $0.6 \text{ GeV}/c$ , and that its direction be within the detector acceptance ( $-0.8660 < \cos\theta < 0.9563$ ), where the missing momentum is defined as the difference between the momentum of the initial  $e^+e^-$  system, and the sum of the observed momentum vectors. The event is subdivided into 3-prong and 1-prong hemispheres with respect to the thrust axis in the CM frame. These are referred to as the signal and tag side, respectively. We allow at most two photons on the tag side to account for initial state radiation, while requiring at most one photon for the  $\ell\phi$ ,  $\ell K^{*0}$ ,  $\ell\bar{K}^{*0}$  modes, and two photons except for  $\pi^0$  daughters for the  $\ell\omega$  modes on the signal side to reduce the  $q\bar{q}$  BG.

We require that the muon likelihood ratio  $P_\mu$  be greater than 0.95 for momentum greater than  $1.0 \text{ GeV}/c$  and the electron likelihood ratio  $P_e$  be greater than 0.9 for momentum greater than  $0.5 \text{ GeV}/c$  for the charged lepton-candidate track on the signal side. Here  $P_x$  is the likelihood ratio for a charged particle of type  $x$  ( $x = \mu, e, K$  or  $\pi$ ), defined as  $P_x = L_x / (\sum_x L_x)$ , where  $L_x$  is the likelihood for particle type  $x$ , determined from the responses of the relevant detectors [11]. The efficiencies for muon and electron identification are 92% for momenta larger than  $1.0 \text{ GeV}/c$  and 94% for momenta larger than  $0.5 \text{ GeV}/c$ .

Candidate  $\phi$  mesons are selected by requiring the invariant mass of  $K^+K^-$  daughters to be in the range  $1.01 \text{ GeV}/c^2 < M_{K^+K^-} < 1.03 \text{ GeV}/c^2$ . We require that both kaon daughters have kaon likelihood ratios  $P_K > 0.8$  and electron likelihood ratios  $P_e < 0.1$  to reduce the background from  $e^+e^-$  conversions. Candidate  $\omega$  mesons are reconstructed from  $\pi^+\pi^-\pi^0$  with the invariant mass requirement  $0.757 \text{ GeV}/c^2 < M_{\pi^+\pi^-\pi^0} < 0.808 \text{ GeV}/c^2$ . The  $\pi^0$  candidate is selected from  $\gamma$  pairs with invariant mass in the range,  $0.11 \text{ GeV}/c^2 < M_{\gamma\gamma} < 0.15 \text{ GeV}/c^2$ . In order to improve the  $\omega$  mass resolution, the  $\pi^0$  mass is constrained to be  $135 \text{ MeV}/c^2$  for the  $\omega$  mass reconstruction. Candidate  $K^{*0}$  and  $\bar{K}^{*0}$  mesons are selected with  $K^\pm\pi^\mp$  invariant mass in the range  $0.827 \text{ GeV}/c^2 < M_{K\pi} < 0.986 \text{ GeV}/c^2$ , and requiring that the kaon daughter have  $P_K > 0.8$  and both daughters have  $P_e < 0.1$ . Figs. 1(a,b,c) show the invariant mass distributions of the  $\phi$ ,  $\omega$  and  $K^{*0}$  candidates for  $\tau^- \rightarrow \mu^-\phi$ ,  $\tau^- \rightarrow \mu^-\omega$  and  $\tau^- \rightarrow \mu^-K^{*0}$ , respectively. The estimated BG distributions agree with the data. The main BG contribution is due to  $q\bar{q}$  events with  $\phi$  mesons for the  $\tau^- \rightarrow \ell^-\phi$  mode,  $\tau^- \rightarrow \pi^-\omega\nu_\tau$  with the pion misidentified as a lepton for the  $\tau^- \rightarrow \ell^-\omega$

TABLE I: Selection criteria using  $p_{\text{miss}}$  (GeV/c) and  $m_{\text{miss}}^2$  ((GeV/c<sup>2</sup>)<sup>2</sup>) where  $p_{\text{miss}}$  is missing momentum and  $m_{\text{miss}}^2$  is missing mass squared.

| Mode                                    | Selection criteria  |
|---|---|
| $\tau^- \rightarrow \ell^- \phi$        | $p_{\text{miss}} > \frac{8}{9} m_{\text{miss}}^2$ and $m_{\text{miss}}^2 > -0.5$                              |
| $\tau^- \rightarrow \ell^- \omega$      | $p_{\text{miss}} > \frac{8}{3} m_{\text{miss}}^2 - \frac{8}{3}$ and $m_{\text{miss}}^2 > -0.5$                |
| $\tau^- \rightarrow \mu^- K^{*0}$       | $p_{\text{miss}} > \frac{8}{4.5} m_{\text{miss}}^2 - \frac{8}{9}$ and $p_{\text{miss}} > 8 m_{\text{miss}}^2$ |
| $\tau^- \rightarrow e^- K^{*0}$         | $p_{\text{miss}} > \frac{8}{5.5} m_{\text{miss}}^2 - \frac{8}{11}$ and $m_{\text{miss}}^2 > 0$                |
| $\tau^- \rightarrow \mu^- \bar{K}^{*0}$ | $p_{\text{miss}} > \frac{8}{6.5} m_{\text{miss}}^2$ and $m_{\text{miss}}^2 > -0.5$                            |
| $\tau^- \rightarrow e^- \bar{K}^{*0}$   | $p_{\text{miss}} > \frac{6}{5} m_{\text{miss}}^2$ and $p_{\text{miss}} > -\frac{8}{1.4} m_{\text{miss}}^2$    |

mode, and  $\tau^- \rightarrow \pi^- \pi^+ \pi^- \nu_\tau$  with one pion misidentified as a kaon and another misidentified as a lepton for the  $\tau^- \rightarrow \ell^- K^{*0}$  and  $\ell^- \bar{K}^{*0}$  modes.

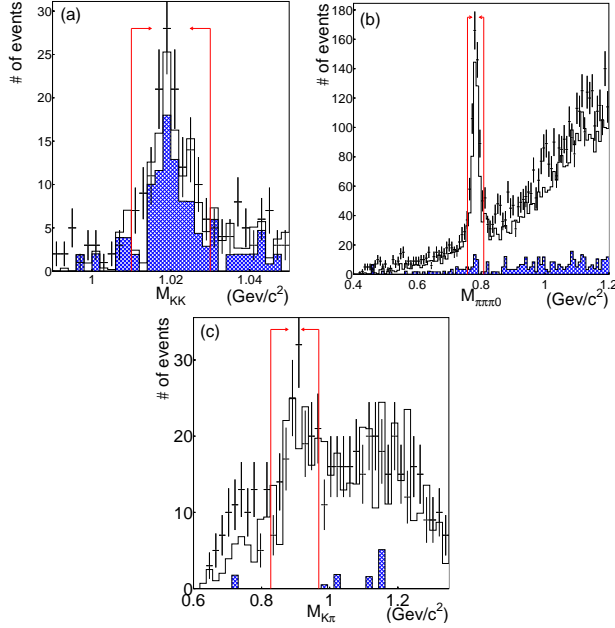


FIG. 1: The mass distribution of (a)  $\phi \rightarrow K^+ K^-$  for  $\tau^- \rightarrow \mu^- \phi$ , (b)  $\omega \rightarrow \pi^+ \pi^- \pi^0$  for  $\tau^- \rightarrow \mu^- \omega$  and (c)  $K^{*0} \rightarrow K^+ \pi^-$  for  $\tau^- \rightarrow \mu^- K^{*0}$  after muon identification. The points with error bars are data. The open histogram shows the expected  $\tau^+ \tau^-$  BG MC and the hatched one  $q\bar{q}$  MC and two-photon MC. The regions between the vertical red lines are selected.

To reduce the remaining BG from  $\tau^+ \tau^-$  and  $q\bar{q}$ , we require the relations between the missing momentum  $p_{\text{miss}}$  (GeV/c) and missing mass squared  $m_{\text{miss}}^2$  ((GeV/c<sup>2</sup>)<sup>2</sup>) summarized in Table I.

For the  $\ell\omega$  ( $\ell K^{*0}$  and  $\ell \bar{K}^{*0}$ ) mode, we require that the opening angle between the lepton and  $\omega$  ( $K^{*0}$ ) on the signal side in the CM frame,  $\theta_{\ell\omega}^{\text{CM}}$  ( $\theta_{\ell K^{*0}}^{\text{CM}}$ ), satisfy  $\cos \theta_{\ell\omega}^{\text{CM}} < 0.88$  ( $\cos \theta_{\ell K^{*0}}^{\text{CM}} < 0.93$ ), respectively. To remove two-photon BG for the  $e\phi$ ,  $e\omega$  and  $eK^{*0}$  ( $\bar{K}^{*0}$ ) modes, we add a condition on an opening angle,  $\alpha$ , between the direction of the total momentum of charged

tracks and  $\gamma$ 's on the signal side and that on the tag side, as  $\cos \alpha > -0.999$ ,  $\cos \alpha > -0.996$  and  $\cos \alpha > -0.990$ , respectively.

To identify signal  $\tau$  decays, we reconstruct the invariant mass of  $\ell V^0$ ,  $M_{\text{inv}}$ , and the energy difference,  $\Delta E$ , between the sum of energies on the signal side and the beam energy  $E_{\text{beam}}$  in the CM frame. Signal events should be distributed around  $M_{\text{inv}} = M_\tau$  and  $\Delta E = 0$ , where  $M_\tau$  is the nominal  $\tau$  mass. For the  $\ell\omega$  modes, we use the beam energy constrained mass  $M_{\text{bc}}$  as the invariant mass  $M_{\text{inv}}$ , where  $M_{\text{bc}} = \sqrt{E_{\text{beam}}^2 - (\vec{p}_\tau)^2}$ , in order to improve the mass resolution, which is smeared due to the  $\gamma$  energy resolution. For the calculation of the  $\tau$  momentum  $\vec{p}_\tau$ , we replace the magnitude of the  $\pi^0$  momentum with the momentum calculated from the beam energy and the energies of charged tracks on the signal side, while we fix the direction of the  $\pi^0$  momentum.

The resolutions in  $\Delta E$  and  $M_{\text{inv}}$  evaluated using the signal MC are summarized in Table II. We define the signal region in the  $\Delta E - M_{\text{inv}}$  plane as a  $\pm 3\sigma$  ellipse. In order to avoid biases in the event selection, we blinded the signal region until the analysis is finalized and used the data in a  $\pm 10\sigma$  sideband box to estimate BG.

TABLE II: Resolutions in  $M_{\text{inv}}$  in MeV/c<sup>2</sup> and  $\Delta E$  in MeV. The superscripts low and high indicate the lower and higher sides of the peak, respectively.

| Mode                                    | $\sigma_{M_{\text{inv}}}^{\text{high}}$ | $\sigma_{M_{\text{inv}}}^{\text{low}}$ | $\sigma_{\Delta E}^{\text{high}}$ | $\sigma_{\Delta E}^{\text{low}}$ |
|---|---|--|-----------------------------------|----------------------------------|
| $\tau^- \rightarrow \mu^- \phi$         | $3.4 \pm 0.2$                           | $3.4 \pm 0.2$                          | $13.2 \pm 0.4$                    | $14.0 \pm 0.5$                   |
| $\tau^- \rightarrow e^- \phi$           | $3.7 \pm 0.1$                           | $3.6 \pm 0.1$                          | $13.3 \pm 0.7$                    | $15.4 \pm 0.7$                   |
| $\tau^- \rightarrow \mu^- \omega$       | $5.9 \pm 0.1$                           | $6.2 \pm 0.1$                          | $19.3 \pm 0.6$                    | $30.3 \pm 0.8$                   |
| $\tau^- \rightarrow e^- \omega$         | $6.1 \pm 0.1$                           | $6.5 \pm 0.1$                          | $20.4 \pm 0.7$                    | $32.5 \pm 1.3$                   |
| $\tau^- \rightarrow \mu^- K^{*0}$       | $4.5 \pm 0.4$                           | $4.5 \pm 0.4$                          | $13.8 \pm 0.3$                    | $14.4 \pm 0.4$                   |
| $\tau^- \rightarrow e^- K^{*0}$         | $4.3 \pm 0.1$                           | $5.1 \pm 0.1$                          | $12.9 \pm 0.3$                    | $18.0 \pm 0.4$                   |
| $\tau^- \rightarrow \mu^- \bar{K}^{*0}$ | $4.7 \pm 0.1$                           | $4.4 \pm 0.1$                          | $14.0 \pm 0.3$                    | $15.0 \pm 0.3$                   |
| $\tau^- \rightarrow e^- \bar{K}^{*0}$   | $4.6 \pm 0.1$                           | $4.9 \pm 0.1$                          | $12.6 \pm 0.6$                    | $17.8 \pm 0.5$                   |

## RESULTS

After all selection requirements, a few events remain in the signal region, as shown in Figs. 2, 3, 4 and 5. For the  $\ell\phi$ ,  $\ell K^{*0}$  and  $\mu \bar{K}^{*0}$  modes, the expected number of BG events in the signal region are estimated using the sideband data, assuming that the BG distribution is flat in the  $\pm 10\sigma$  box. For the  $\mu\omega$  modes, we estimate the BG contribution in the signal region using the BG MC distribution normalized to the ratio of data and MC in the sideband region, because a rather large number of BG events remain, which are mainly from  $\tau^- \rightarrow \pi^- \omega \nu_\tau$ . For the  $\tau^- \rightarrow e^- \omega$  and  $e^- \bar{K}^{*0}$  modes, since no events remain in the  $\pm 10\sigma$  box for data, the number of expected BG events in the signal region is zero. We calculate the error

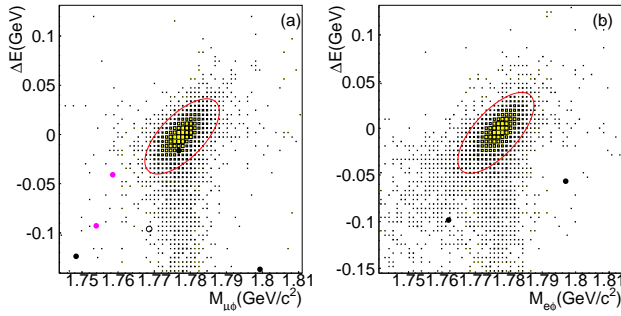


FIG. 2:  $\Delta E$  vs.  $M_{\text{inv}}$  distributions for (a)  $\tau^- \rightarrow \mu^- \phi$  and (b)  $\tau^- \rightarrow e^- \phi$ , after all selection criteria. Dots are data, yellow boxes show the signal MC, purple dots are background from  $\tau \rightarrow \phi \pi \nu$  MC and open circles show other  $\tau$ -pair backgrounds. The elliptical area is the  $3\sigma$  signal region.

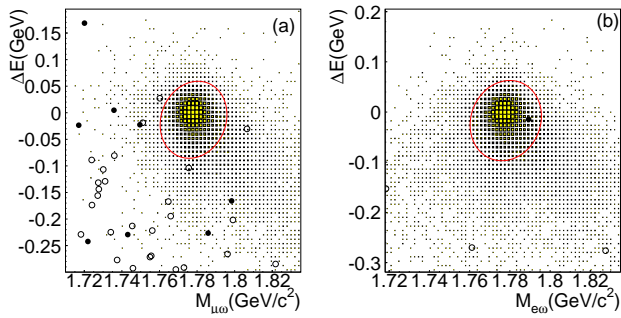


FIG. 3:  $\Delta E$  vs.  $M_{\text{inv}}$  distributions for (a)  $\tau^- \rightarrow \mu^- \omega$  and (b)  $\tau^- \rightarrow e^- \omega$ , after all selection criteria. Dots are data, yellow boxes show the signal MC, and open circles show  $\tau$ -pair background MC. The elliptical area is the  $3\sigma$  signal region.

from the number of remaining MC events in the  $\pm 10\sigma$  box assuming a flat BG distribution. The number of events in the  $\pm 10\sigma$  box excluding the signal region and the number of the expected BG events are listed in Tables III and IV. The comparison between the data and MC shows reasonable agreement; the BG is suppressed well by the event selection.

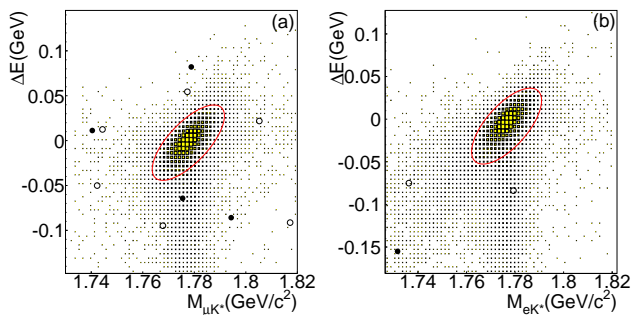


FIG. 4:  $\Delta E$  vs.  $M_{\text{inv}}$  distributions for (a)  $\tau^- \rightarrow \mu^- K^{*0}$  and (b)  $\tau^- \rightarrow e^- K^{*0}$ , after all selection criteria. Dots are data, yellow boxes show the signal MC and open circles show  $\tau$ -pair background MC. The elliptical area is the  $3\sigma$  signal region.

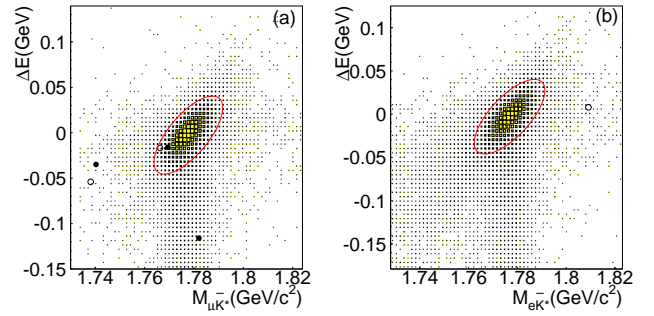


FIG. 5:  $\Delta E$  vs.  $M_{\text{inv}}$  distributions for (a)  $\tau^- \rightarrow \mu^- \bar{K}^{*0}$  and (b)  $\tau^- \rightarrow e^- \bar{K}^{*0}$ , after all selection criteria. Dots are data, yellow boxes show the signal MC and open circles show  $\tau$ -pair background MC. The elliptical area is the  $3\sigma$  signal region.

TABLE III: Number of events in the sideband region.

| Mode                                    | $N_{\text{ev}}$ in the $\pm 10\sigma$ box in the sideband region |                 |
|---|--|-----------------|
|   | data   | MC              |
| $\tau^- \rightarrow \mu^- \phi$         | 2  | $1.68 \pm 1.17$ |
| $\tau^- \rightarrow e^- \phi$           | 2  | 0               |
| $\tau^- \rightarrow \mu^- \omega$       | 8  | $8.97 \pm 1.72$ |
| $\tau^- \rightarrow e^- \omega$         | 0  | $1.07 \pm 0.62$ |
| $\tau^- \rightarrow \mu^- K^{*0}$       | 4  | $3.94 \pm 1.61$ |
| $\tau^- \rightarrow e^- K^{*0}$         | 1  | $1.58 \pm 1.11$ |
| $\tau^- \rightarrow \mu^- \bar{K}^{*0}$ | 2  | $0.90 \pm 1.11$ |
| $\tau^- \rightarrow e^- \bar{K}^{*0}$   | 0  | $0.06 \pm 0.06$ |

From the remaining number of data events in the signal region and the number of expected BG events, we evaluated the upper limit  $s_{90}$  on the number of signal events at 90% CL with systematic uncertainties included in the Feldman-Cousins method [12] using the POLE code [13]. The main systematic uncertainties on the detection efficiency come from track reconstruction (1.0% per track), electron identification (2.2%), muon identification (2.0%), kaon identification (1.4% for  $\phi$  reconstruction).

TABLE IV: Number of expected BG events.

| Mode                                    | $N_{\text{ev}}$ of expected BG in the signal region |
|---|---|
| $\tau^- \rightarrow \mu^- \phi$         | $0.11 \pm 0.08$                                     |
| $\tau^- \rightarrow e^- \phi$           | $0.11 \pm 0.08$                                     |
| $\tau^- \rightarrow \mu^- \omega$       | $0.19 \pm 0.21$                                     |
| $\tau^- \rightarrow e^- \omega$         | $0 \pm 0.07$  |
| $\tau^- \rightarrow \mu^- K^{*0}$       | $0.22 \pm 0.11$                                     |
| $\tau^- \rightarrow e^- K^{*0}$         | $0.05 \pm 0.05$                                     |
| $\tau^- \rightarrow \mu^- \bar{K}^{*0}$ | $0.10 \pm 0.07$                                     |
| $\tau^- \rightarrow e^- \bar{K}^{*0}$   | $0 \pm 0.02$  |

tion and 1.1% for  $K^{*0}$ ,  $\pi^0$  reconstruction (4.0%), statistics of the signal MC (1.3% for  $\ell\phi$ , 0.7% for  $\ell\omega$  and 0.6% for  $\ell K^{*0}$  and  $\ell\bar{K}^{*0}$ ) and uncertainties in the branching fractions for  $\phi \rightarrow K^+K^-$  and  $\omega \rightarrow \pi^+\pi^-\pi^0$  (1.2% and 0.8%). The uncertainty in the number of  $\tau$ -pair events mainly comes from the luminosity measurement (1.4%).

Upper limits on the branching fractions  $\mathcal{B}$  are calculated as  $\mathcal{B} < \frac{s_{90}}{2N_{\tau\tau}\epsilon}$ , where  $N_{\tau\tau} = 4.99 \times 10^8$ , which we calculate using cross section of 0.919 nb according to [14], is the total number of the  $\tau$ -pairs produced and  $\epsilon$  is the signal efficiency including the branching fractions of  $\phi \rightarrow K^+K^-$ ,  $\omega \rightarrow \pi^+\pi^-\pi^0$  and  $K^{*0} \rightarrow K^+\pi^-$  [15]. The resulting upper limits on the branching fractions are summarized in Table V.

TABLE V: Summary of the number of observed events  $N_{\text{obs}}$ , detection efficiency  $\epsilon$ , total systematic error  $\Delta\epsilon/\epsilon$ , 90% CL upper limit of signal events  $s_{90}$  and 90% CL upper limit of branching fractions.

| Mode                                    | $N_{\text{obs}}$ | $\epsilon$ | $\Delta\epsilon/\epsilon$ | $s_{90}$ | UL on BF<br>(90% CL) |
|---|------------------|------------|---------------------------|----------|----------------------|
| $\tau^- \rightarrow \mu^- \phi$         | 1                | 3.14       | 5.2                       | 4.21     | $1.3 \times 10^{-7}$ |
| $\tau^- \rightarrow e^- \phi$           | 0                | 3.10       | 5.3                       | 2.34     | $7.6 \times 10^{-8}$ |
| $\tau^- \rightarrow \mu^- \omega$       | 0                | 2.51       | 6.3                       | 2.25     | $9.0 \times 10^{-8}$ |
| $\tau^- \rightarrow e^- \omega$         | 1                | 2.46       | 6.3                       | 4.34     | $1.8 \times 10^{-7}$ |
| $\tau^- \rightarrow \mu^- K^{*0}$       | 0                | 3.71       | 4.8                       | 2.24     | $6.1 \times 10^{-8}$ |
| $\tau^- \rightarrow e^- K^{*0}$         | 0                | 3.04       | 4.9                       | 2.42     | $8.0 \times 10^{-8}$ |
| $\tau^- \rightarrow \mu^- \bar{K}^{*0}$ | 1                | 4.02       | 4.8                       | 4.23     | $1.1 \times 10^{-7}$ |
| $\tau^- \rightarrow e^- \bar{K}^{*0}$   | 0                | 3.21       | 4.9                       | 2.45     | $7.7 \times 10^{-8}$ |

## SUMMARY

We have searched for LFV decays  $\tau^- \rightarrow \ell^- \phi$ ,  $\ell^- \omega$ ,  $\ell^- K^{*0}$  and  $\ell^- \bar{K}^{*0}$  using a  $543 \text{ fb}^{-1}$  data sample from the Belle experiment. No evidence for a signal is observed and upper limits on the branching fractions are set in the range  $(0.6 - 1.8) \times 10^{-7}$  at the 90% confidence level. This analysis is the first search for  $\tau \rightarrow \ell\omega$  modes. The results for the  $\tau^- \rightarrow \ell^- \phi$ ,  $\ell^- K^{*0}$  and  $\ell^- \bar{K}^{*0}$  modes are 3.6–9.6 times more restrictive than our previous results obtained using  $158 \text{ fb}^{-1}$  of data. The sensitivity improvement includes a factor of 3.4 in data statistics and an optimized analysis with higher efficiency and much improved BG suppression. The improved upper limits can be used to constrain the parameter spaces of various scenarios beyond the SM.

## ACKNOWLEDGEMENTS

We thank the KEKB group for the excellent operation of the accelerator, the KEK cryogenics group for the

efficient operation of the solenoid, and the KEK computer group and the National Institute of Informatics for valuable computing and Super-SINET network support. We acknowledge support from the Ministry of Education, Culture, Sports, Science, and Technology of Japan and the Japan Society for the Promotion of Science; the Australian Research Council and the Australian Department of Education, Science and Training; the National Science Foundation of China and the Knowledge Innovation Program of the Chinese Academy of Sciences under contract No. 10575109 and IHEP-U-503; the Department of Science and Technology of India; the BK21 program of the Ministry of Education of Korea, the CHEP SRC program and Basic Research program (grant No. R01-2005-000-10089-0) of the Korea Science and Engineering Foundation, and the Pure Basic Research Group program of the Korea Research Foundation; the Polish State Committee for Scientific Research; the Ministry of Education and Science of the Russian Federation and the Russian Federal Agency for Atomic Energy; the Slovenian Research Agency; the Swiss National Science Foundation; the National Science Council and the Ministry of Education of Taiwan; and the U.S. Department of Energy.

- [1] A. Ilakovac, Phys. Rev. D **62**, 036010 (2000).
- [2] A. Brignole and A. Rossi, Nucl. Phys. B **701**, 3 (2004).
- [3] C.-H. Chen and C.-Q. Geng, Phys. Rev. D **74**, 035010 (2006).
- [4] Throughout this paper, the inclusion of the charge-conjugate decay modes is implied unless otherwise stated.
- [5] D.W. Bliss *et al.* (CLEO Collab.), Phys. Rev. D **57**, 5903 (1998).
- [6] Y. Yusa *et al.* (Belle Collab.), Phys. Lett. B **640**, 138 (2006).
- [7] A. Abashian *et al.* (Belle Collab.), Nucl. Instr. and Meth. A **479**, 117 (2002).
- [8] S. Kurokawa and E. Kikutani, Nucl. Instr. and Meth. A **499**, 1 (2003), and other papers included in this volume.
- [9] Z. Natkaniec *et al.* (Belle SVD2 Group), Nucl. Instr. and Meth. A **560**, 1 (2006).
- [10] S. Jadach, B.F.L. Ward, Z. Wąs, Comp. Phys. Commun. **130**, 260 (2000).
- [11] K. Hanagaki *et al.*, Nucl. Instr. and Meth. A **485**, 490 (2002); A. Abashian *et al.*, Nucl. Instr. and Meth. A **491**, 69 (2002).
- [12] G. J. Feldman and R. D. Cousins, Phys. Rev. D **57**, 3873 (1998).
- [13] The Highland-Cousins method for calculating upper limits with systematic errors is described in J. Conrad *et al.*, Phys. Rev. D **67**, 012002 (2003).
- [14] S. Banerjee, B. Pietrzyk, J.M. Roney and Z. Wąs, arXiv:0706.3235 [hep-ex].
- [15] W.-M. Yao *et al.* (Particle Data Group), J. Phys. G **33**, 1 (2006).